Cell Reports
Article

Visual Map Shifts based on Whisker-Guided Cues in the Young Mouse Visual Cortex

Kohei Yoshitake,[1,3] Hiroaki Tsukano,[1] Manavu Tohmi,[1] Seiji Komagata,[1] Ryuichi Hishida,[1] Takeshi Yagi,[2,3] and Katsuei Shibuki[1,3,*]

[1]Department of Neurophysiology, Brain Research Institute, Niigata University, 1-757 Asahi-machi, Chuo-ku, Niigata 951-8585, Japan
[2]KOKORO-Biology Group, Laboratories for Integrated Biology, Graduate School of Frontier Biosciences, Osaka University, 1-3 Yamadaoka, Suita, Osaka 565-0871, Japan
[3]Japan Science and Technology Agency, CREST, 7 Goban-cho, Chiyoda-ku, Tokyo 102-0076, Japan
*Correspondence: shibuki@bri.niigata-u.ac.jp
http://dx.doi.org/10.1016/j.celrep.2013.11.006

SUMMARY

Mice navigate nearby space using their vision and whiskers, and young mice learn to integrate these heterogeneous inputs in perceptual space. We found that cortical responses were depressed in the primary visual cortex of young mice after wearing a monocular prism. This depression was uniformly observed in the primary visual cortex and was eliminated by whisker trimming or lesions in the posterior parietal cortex. Compensatory visual map shifts of responses elicited via the eye that had worn the prism were also observed. As a result, cortical responses elicited via each eye were clearly separated when a visual stimulus was placed in front of the mice. A comparison of response areas before and after prism wearing indicated that the map shifts were produced by depression with spatial eccentricity. Visual map shifts based on whisker-guided cues may serve as a model for investigating the cellular and molecular mechanisms underlying higher sensory integration in the mammalian brain.

INTRODUCTION

Mice navigate their surrounding space using information derived from their whiskers as well as visual information (Diamond et al., 2008), and behaving mice experience coactivated visual and whisker inputs on many occasions. Young mice with growing body parts must learn to adjust spatial information obtained from the eyes to the whisker input, which is processed in the barrel cortex established before eye opening (O'Leary et al., 1994). However, the mechanisms involved in achieving this are unknown. An example of neural plasticity induced by a modified relationship between cross-modal sensory inputs is an auditory map shift in the superior colliculus of barn owls wearing prism goggles (Knudsen, 2002; McBride et al., 2008). The auditory localization cues in barn owls are the relative timing and level of sound at both ears, and these cues are translated to localize the sound sources using visual information (Konishi, 2003). Therefore, the auditory localization maps in barn owls are strongly affected by modified alignment of visual information caused by prism goggles (Knudsen, 2002; McBride et al., 2008). Sound localization in auditory space is also distorted in humans with hemianopia (Lewald et al., 2009). These results raise the possibility that cortical responses in the primary visual cortex (V1) of young mice could be affected by artificially uncorrelated visual and whisker inputs. In the present study, we tested this cross-modal plasticity in young mice that wore a monocular prism goggle.

Ocular dominance plasticity in V1 is induced by unbalanced binocular inputs during monocular deprivation (MD) in the early critical period (Gordon and Stryker, 1996; Hensch, 2005; Tohmi et al., 2006) and later periods (Sawtell et al., 2003; Tagawa et al., 2005). Artificially uncorrelated binocular inputs caused by strabismus induce other types of ocular dominance plasticity, such as a reduction in the number of binocularly driven neurons and amblyopia (Maffei and Bisti, 1976; Zhang et al., 2005; Sengpiel et al., 2006; Hess et al., 2010). Ocular dominance plasticity is induced only in the binocular region of V1 (V1B). However, although a form of intrinsic plasticity is present in the monocular region of V1 (V1M) throughout the critical period, it is only transiently expressed at the onset of the critical period in V1B (Nataraj and Turrigiano, 2011). Reduced visual input induces a certain type of cross-modal plasticity in which neurons in V1B and V1M are driven by nonvisual sensory inputs (Bavelier and Neville, 2002; Van Brussel et al., 2011). Therefore, another type of cross-modal plasticity may be induced in V1B and V1M, when visual input is uncorrelated to whisker input in young mice.

In carnivores and primates, V1 neurons transmit specific information to higher visual areas, which are divided into dorsal pathways that are specialized to process motion and spatial relationships, and ventral pathways that are specialized to process detailed shapes and patterns in an image (Van Essen and Gallant, 1994). The dorsal pathways are connected to the posterior parietal cortex (PPC), where visual information is integrated with somatosensory information for recognition of the space around the subject (Andersen, 1997; Maravita et al., 2003). The PPC also plays an important role in spatial working memory

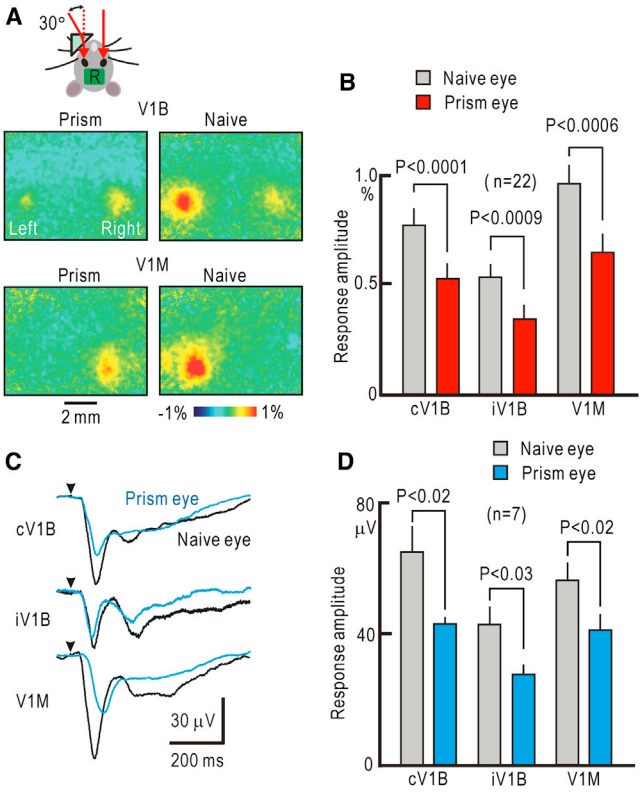

Figure 1. Prism-Induced Cortical Depression in V1B and V1M

(A) Cortical responses elicited by LED stimuli in V1B (upper panels) and V1M (lower panels) via the left eye, which had worn the prism goggle (left panels) or via the right, naive eye (right panels). The inset shows the prism goggle attached to the head of a mouse ("R" shows the imaged area). Cortical responses elicited via the left eye were depressed compared with those elicited via the right eye.

(B) Response amplitudes in $\Delta F/F_0$ (mean and SEM) in the contralateral V1B (cV1B), ipsilateral V1B (iV1B), and contralateral V1M.

(C) Field potential recordings at the center of the response area identified by imaging. Arrowheads represent stimulus onset. Responses elicited via the left eye (blue traces) were depressed compared with those elicited via the right eye (black traces).

(D) Response amplitudes of field potentials. The images and traces shown in (A) and (C), respectively, were obtained from a representative animal. Group data are shown in (B) and (D).

See also Figure S1.

(Harvey et al., 2012). In mice, V1 neurons are characterized by the absence of functional clustering with respect to orientation preference (Ohki et al., 2005) or ocular dominance (Mrsic-Flogel et al., 2007). However, recent studies using two-photon microscopy have revealed the presence of dorsal and ventral pathways in mice (Andermann et al., 2011; Marshel et al., 2011). Therefore, visual information mediated via the dorsal pathways of mice may be conveyed to the PPC and integrated with somatosensory information in a cross-modal association area of the PPC (Pinto-Hamuy et al., 2004; Rogers and Kesner, 2007; Torrealba and Valdés, 2008; Wang et al., 2011; Olcese et al., 2013). Therefore, PPC may play essential roles in the cross-modal cortical plasticity in V1. In the present study, we also tested this possibility.

RESULTS

Prism-Induced Cortical Depression in V1B and V1M

We produced an artificial misalignment between whisker and visual inputs in a mouse using a monocular prism goggle that bent the path of light by 30° (Figure 1A, inset). This goggle was attached to the head of a 4-week-old mouse for 5–7 days. After the mouse was anesthetized with urethane (1.6 g/kg, i.p.) and the goggle was removed, cortical responses in V1 to LED stimuli were recorded by transcranial flavoprotein fluorescence imaging (Tohmi et al., 2006). Cortical responses in V1B were elicited by LED stimuli, placed at 0° in the horizontal plane, via the left eye, which had worn the prism (Figure 1A, upper left panel). These responses were significantly depressed compared with those elicited via the right, naive eye (Figure 1A, upper right). The cortical responses in V1M to LED stimuli placed at 90° on the left side of the mouse (Figure 1A, left lower) were similarly depressed compared with the cortical responses to LED stimuli on the right side (Figure 1A, lower right). The amplitudes of the cortical responses in $\Delta F/F_0$ to each eye were measured in the contralateral V1B, ipsilateral V1B, and contralateral V1M. These results indicate that prism-induced depression was induced in V1M as well as in V1B (Figure 1B). To confirm the findings obtained by flavoprotein fluorescence imaging, we made a small hole in the skull over the fluorescence response areas and recorded field potentials through a glass micropipette inserted into the response center, at which a local $\Delta F/F_0$ change was maximal, to a depth of 400 μm from the pial surface. Field potential traces (Figure 1C) showed that the prism-induced cortical depression was also observed as changes in field potential amplitudes (Figure 1D).

We further investigated the properties of prism-induced cortical depression in V1. The cortical fluorescence responses to grating patterns were also depressed after prism wearing (Figures S1A and S1B). No cortical depression was found when the prism goggle was attached to the heads of mice for 7 days between 6 and 7 weeks of age (Figure S1C), indicating the presence of a critical period comparable to that of ocular dominance plasticity after MD (Gordon and Stryker, 1996; Hensch, 2005; Tohmi et al., 2006). However, ocular dominance plasticity after MD was observed only in V1B (for example, see Figure S1D), indicating that the two types of cortical plasticity are different from each other.

Role of Whiskers in Prism-Induced Cortical Depression

The prism-induced cortical depression in the present study might be produced by the abnormal visual experience alone rather than by visuotactile spatial misalignment. To exclude this possibility, we deprived the mice of sensory information obtained via the whiskers by trimming the whiskers (Figure 2A, inset). No apparent prism-induced cortical depression was found in mice with trimmed whiskers (Figures 2A and 2B), suggesting that sensory information obtained via the whiskers played an essential role in inducing the prism-induced cortical depression. In contrast, ocular dominance plasticity after MD was found in mice with trimmed whiskers (Figures 2C and 2D) and visual responses were not clearly affected by whisker

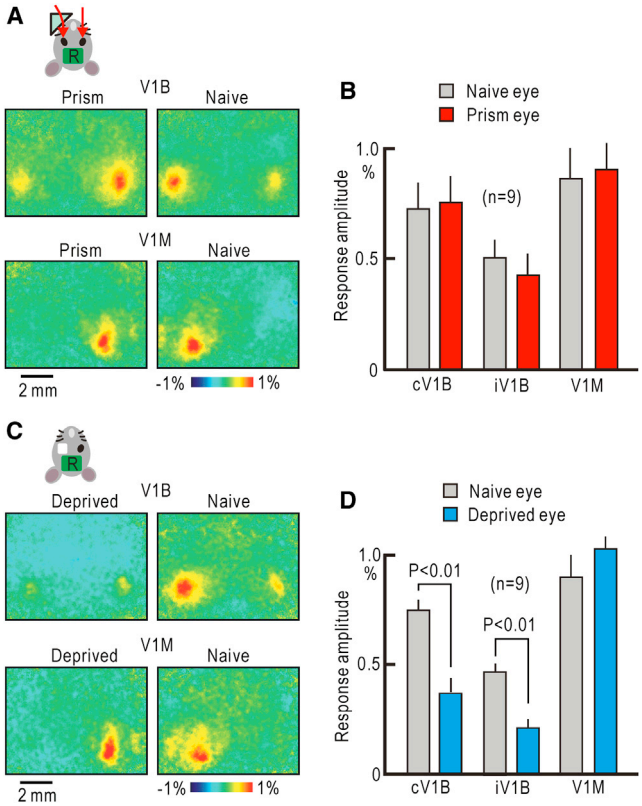

Figure 2. Effects of Whisker Trimming on Prism-Induced Cortical Depression

(A) Cortical responses in mice with trimmed whiskers after prism wearing. Inset shows schematic drawing of the experiment. The prism goggle failed to induce cortical depression in V1.

(B) Response amplitudes in V1B and V1M after prism wearing.

(C) Cortical responses in mice with trimmed whiskers after MD. The inset shows a schematic drawing of the experiment. MD induced cortical depression in V1B.

(D) Response amplitudes in V1B and V1M after MD.

See also Figure S2.

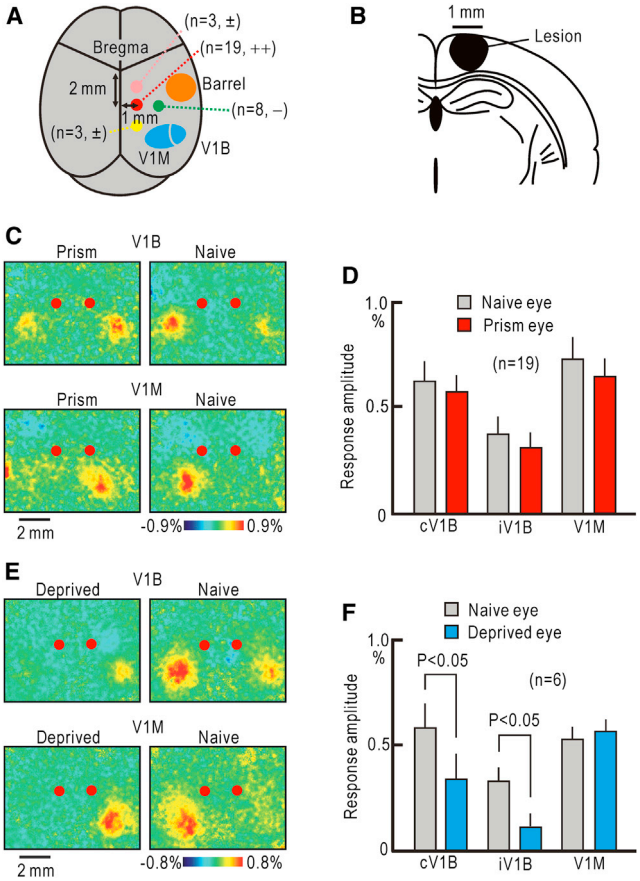

Figure 3. Effects of PPC Lesioning on Prism-Induced Cortical Depression

(A) The lesioned cortical site (red spot with "++") that significantly suppressed the prism-induced cortical depression in 19 mice. Nearby sites were tested at 1 mm intervals with no effect (green spot with "–" in eight mice) or mild suppression (yellow and pink spots with "±" in three mice each).

(B) Schematic drawing of the effective lesion in a coronal section.

(C) Cortical responses after prism wearing in mice with bilateral PPC lesions (red spots). No prism-induced depression was found.

(D) Response amplitudes in V1B and V1M after prism wearing. The lesion was made in the right hemispheres of 12 mice and both hemispheres of seven other mice. Since no apparent difference was found between them, the data were mixed.

(E) Cortical responses after MD in mice with bilateral PPC lesions (red spots).

(F) Response amplitudes in V1B and V1M after MD.

See also Figure S3.

trimming alone (Figures S2A and S2B), indicating that whisker trimming had no direct effect on the visual responses in V1.

Similar depression was also induced by spatial misalignment between curled whiskers and a naive eye, and the response area, in which $\Delta F/F_0$ was larger than half the maximal amplitude, was significantly reduced compared with that of the contralateral side (Figures S2C–S2F). These findings strongly suggest that visuotactile spatial misalignment, rather than abnormal visual information, was responsible for inducing the prism-induced cortical depression in response area sizes as well as in response amplitudes.

Role of Higher Cortical Areas in Prism-Induced Cortical Depression

The contribution of whisker input to the induction of prism-induced cortical depression indicates that whisker input was mediated to V1. However, the pathways are unknown. The whisker input might be projected directly to V1, or integrated with visual input in a visuotactile area of the PPC (Pinto-Hamuy et al., 2004; Rogers and Kesner, 2007; Torrealba and Valdés, 2008; Olcese et al., 2013). We tested the latter possibility by producing small electrical lesions in various cortical sites around the PPC at 1 mm intervals (Figures 3A and 3B) and investigated the effects of prism wearing in these mice. When the lesion was made bilaterally or ipsilaterally at 2 mm posterior and 1 mm lateral to the bregma (red spot in Figure 3A), the prism-induced cortical depression was almost completely abolished (Figures 3C and 3D). After lesioning at 2 mm posterior and 2 mm lateral to the bregma (green spot in Figure 3A), depression of the

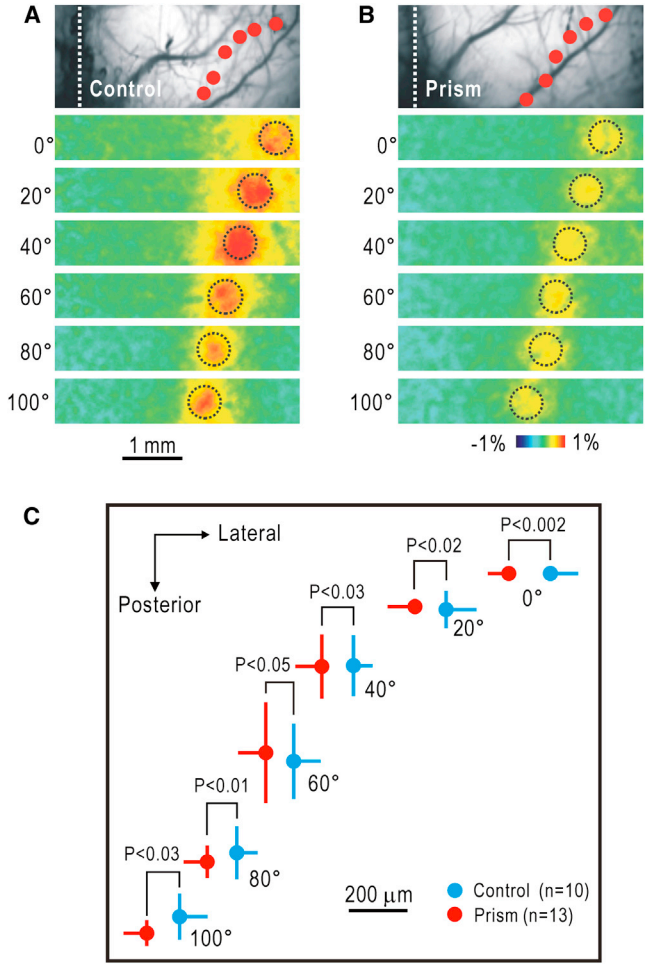

Figure 4. Retinotopic Map Shifts in V1 after Prism Wearing

(A) Cortical responses in the right V1 of a control mouse elicited by LED stimuli placed between 0° and 100° at 20° intervals in the left horizontal plane. The uppermost panel shows the original fluorescence image with red spots at the response centers. The dotted line represents the midline of the superior sagittal sinus. Lower panels show each visual response and the circular window (diameter: 20 pixels) at which $\Delta F/F_0$ was maximal.

(B) Cortical responses in the right V1 of a mouse that had worn the prism goggle.

(C) Comparison of response locations between control mice and mice that had worn the prism goggle. The mediolateral location was measured as the horizontal distance from the midline of the superior sagittal sinus. The anteroposterior location was measured as the vertical distance from the center of the responses elicited by LED placed at 0°.

See also Figure S4.

cortical responses elicited via the left eye normalized to those elicited via the right eye was clearly observed (normalized amplitudes in V1M: 48% ± 13%, mean ± SEM, n = 8; contralateral V1B: 47% ± 10%; ipsilateral V1B: 72% ± 29%). After lesioning at 3 mm posterior and 1 mm lateral (yellow spot in Figure 3A), the depression was mild (V1M: 67% ± 18%, n = 3; contralateral V1B: 78% ± 6%; ipsilateral V1B: 54% ± 11%). After lesioning at 1 mm posterior and 1 mm lateral (pink spot in Figure 3A), the depression was also mild or absent (V1M: 76% ± 18%, n = 3; contralateral V1B: 77% ± 7%; ipsilateral V1B: 110% ± 9%). Ocular dominance plasticity after MD was not abolished by the lesions (Figures 3E and 3F), indicating that the local neural circuits in V1 were not directly impaired by the lesions.

Clustered protocadherins are neuron-specific cell adhesion molecules (Kohmura et al., 1998; Yagi, 2013), and cortico-cortical pathways between the primary somatosensory cortices in both hemispheres are impaired in protocadherin-α constant region knockout (Pcdh-α KO) mice (Yamashita et al., 2012). Since cortico-cortical pathways involving the PPC are likely to play a critical role in visuotactile sensory association, we tested prism-induced depression in Pcdh-α KO mice (Figure S3). Whereas prism-induced depression was not observed (Figures S3A and S3B), ocular dominance plasticity was induced by MD (Figures S3C and S3D). Orientation/direction selectivity of V1 neurons was apparently normal in Pcdh-α KO mice (Figures S3E–S3G). At present, it is unknown how Pcdh-α is involved in the induction of prism-induced cortical depression. However, similarities in phenotypes between mice with PPC lesions and Pcdh-α KO mice suggest that Pcdh-α might be required for PPC functions.

Prism-Induced Map Shifts in V1

Cortical depression in V1 alone cannot eliminate a visuotactile spatial misalignment between visual and whisker inputs. However, skewed depression or shrinkage of the response area with spatial eccentricity and the resulting map shifts may alleviate the visuotactile spatial misalignment. To test this possibility, we investigated the location of visual responses elicited by LED stimuli placed in the left horizontal plane between 0° and 100° at 20° intervals in control mice and mice that had worn the prism goggle (Figures 4A and 4B). These results suggested a more or less uniform medial shift of cortical responses in V1B and V1M of mice that had worn the prism goggle (Figure 4C). In contrast, the acute optical effects of prism wearing were heterogeneous on V1 (Figures S4A–S4C). The areas that were originally responsive to stimuli shown between −10° and 30° received visual inputs shifted by 30°. However, the areas that were responsive to stimuli shown at ≥80° received direct visual inputs that were not disturbed by the prism. The areas that were originally responsive to stimuli between 30° and 80° could not be stimulated via the prism, indicating that they received only diffuse visual inputs through the rough surface of the prism. We also investigated the relationship between the map shift distance and the magnitude of the depression, and found a positive correlation between these two parameters (Figure S4D).

Effects Produced by Prism Wearing in V1B and V1M

Ocular dominance columns have not been found in V1B of mice (Mrsic-Flogel et al., 2007). However, uniform medial shifts of visual responses in the wide areas including V1B suggest the possibility that separation of visual responses elicited via each eye could be produced in V1B after prism wearing. In a control mouse, visual responses elicited via each eye were located in almost the same areas in V1B (Figure 5A). However, the responses were clearly separated in V1B of mice that had worn the prism goggle (Figure 5B). The horizontal distance between visual responses elicited via each eye was significantly larger

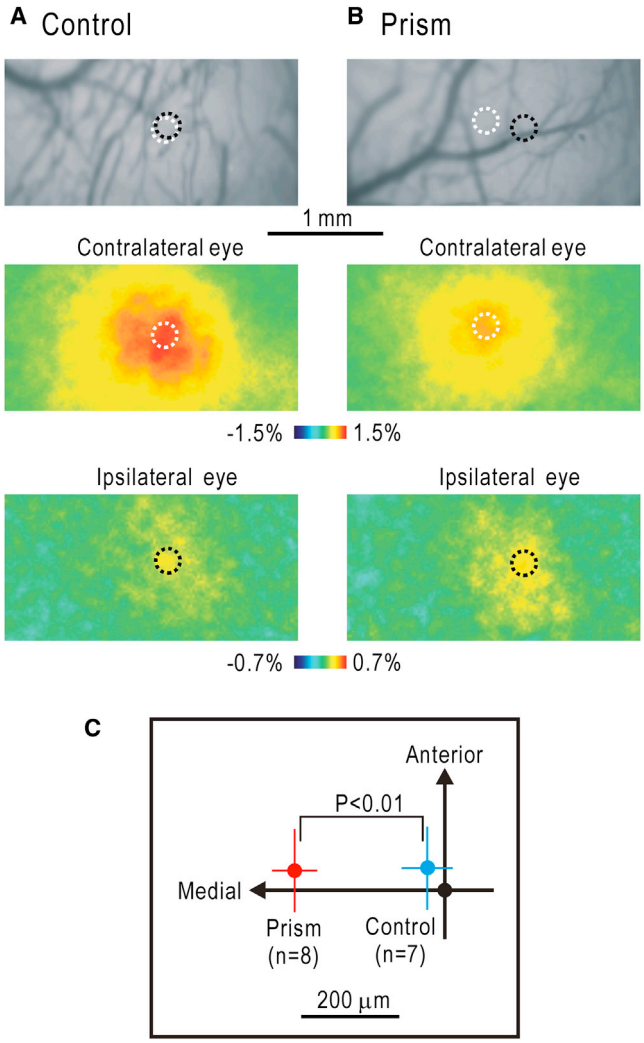

Figure 5. Separation of Visual Responses Elicited via Each Eye in V1B after Prism Wearing

(A) Visual responses stimulated by LED stimuli at 0° via the contralateral eye and the ipsilateral eye in the right V1B of a control mouse. The circular windows (diameter: 10 pixels), at which $\Delta F/F_0$ was maximal, are superimposed on the original fluorescence image in the uppermost panel. This diameter was selected to localize the visual responses elicited via the ipsilateral eye precisely.

(B) Visual responses stimulated via the contralateral eye and the ipsilateral eye in the right V1B of a mouse that had worn the prism goggle.

(C) Locations of the responses elicited via the contralateral eye relative to those of the responses elicited via the ipsilateral eye in control mice and mice that had worn the prism goggle.

See also Figure S5.

in mice that had worn the prism goggle compared with control mice (Figure 5C). These results clearly indicate that ocular dominance column-like structures may be formed even in mice under certain environmental conditions.

V1M areas that responded to stimuli at 90° in the horizontal plane showed depression of visual responses after prism wearing, and this depression is apparently similar to amblyopia in strabismus (Maffei and Bisti, 1976; Zhang et al., 2005; Sengpiel et al., 2006; Hess et al., 2010). Therefore, reduced visual acuity in V1M could be produced, although these areas did not receive abnormal visual inputs disturbed by the prism. We tested this possibility by investigating the flavoprotein fluorescence responses to grating patterns of various spatial frequencies (Figure S5). The results clearly indicated that reduced visual acuity was produced in a part of V1M that had received normal visual inputs.

Comparison of Response Areas before and after Prism Wearing in the Same Mice

The positive correlation between the map shift distance and the magnitude of the depression (Figure S4D) suggests that both changes were intimately related to each other. If visual responses are depressed with spatial eccentricity after prism wearing, map shifts can be produced as a result. To test this possibility, we designed a monocular prism goggle that produced a clockwise or counterclockwise rotation of the path of light to V1M by 20° (Figure 6A), and compared the precise response area in V1M before and after prism wearing in the same mice. To determine the response areas, we investigated periodic visual responses to LED stimuli repeated at 0.25 Hz by performing a Fourier analysis of the imaged signals (Kalatsky and Stryker, 2003). Mice were anesthetized with a mixture of urethane and pentobarbital (0.6 g/kg and 30 mg/kg, i.p., respectively) for reproducible recording and quick recovery afterward. The response center, which was defined as the location of the pixel with the maximal $\Delta F/F_0$, did not shift on the surface of V1 after clockwise prism wearing for 1 week, judging from the relative position of the response center to nearby blood vessels (Figures 6B and 6C). Therefore, the resting eye position in anesthetized mice was unlikely to shift after clockwise prism wearing. However, the lateral (but not the medial) margin of the responsive area, at which the half-maximal $\Delta F/F_0$ was recorded, shrunk by approximately 0.3 mm (Figures 6B–6D). In contrast, the medial (but not the lateral) margin of the responsive area shrunk by approximately 0.2 mm after counterclockwise prism wearing (Figures 6E–6G). Since no comparable change was found in mice that did not wear a goggle (Figures S6A–S6C), we concluded that the skewed shrinkage of the response area was not a result of normal development, but was artificially induced by the visuotactile spatial misalignment. A shift by 20° in the visual field corresponds to a shift of approximately 0.3 mm in the retinotopic map of V1 (Tohmi et al., 2006), so the shrinkage found in the present study compensated for a small but substantial part of the visuotactile spatial misalignment produced by prism wearing. The skewed changes in the response areas after prism wearing strongly suggest that the map shifts are nothing more than a prism-induced cortical depression with spatial eccentricity.

DISCUSSION

Flavoprotein Fluorescence Imaging

The present study was performed with the use of transcranial flavoprotein fluorescence imaging (Tohmi et al., 2009). Flavoprotein fluorescence signals are resistant to photobleaching (Kubota et al., 2008) and are proportional to the amplitudes of neural activity, as shown in Figures 1B and 1D and in

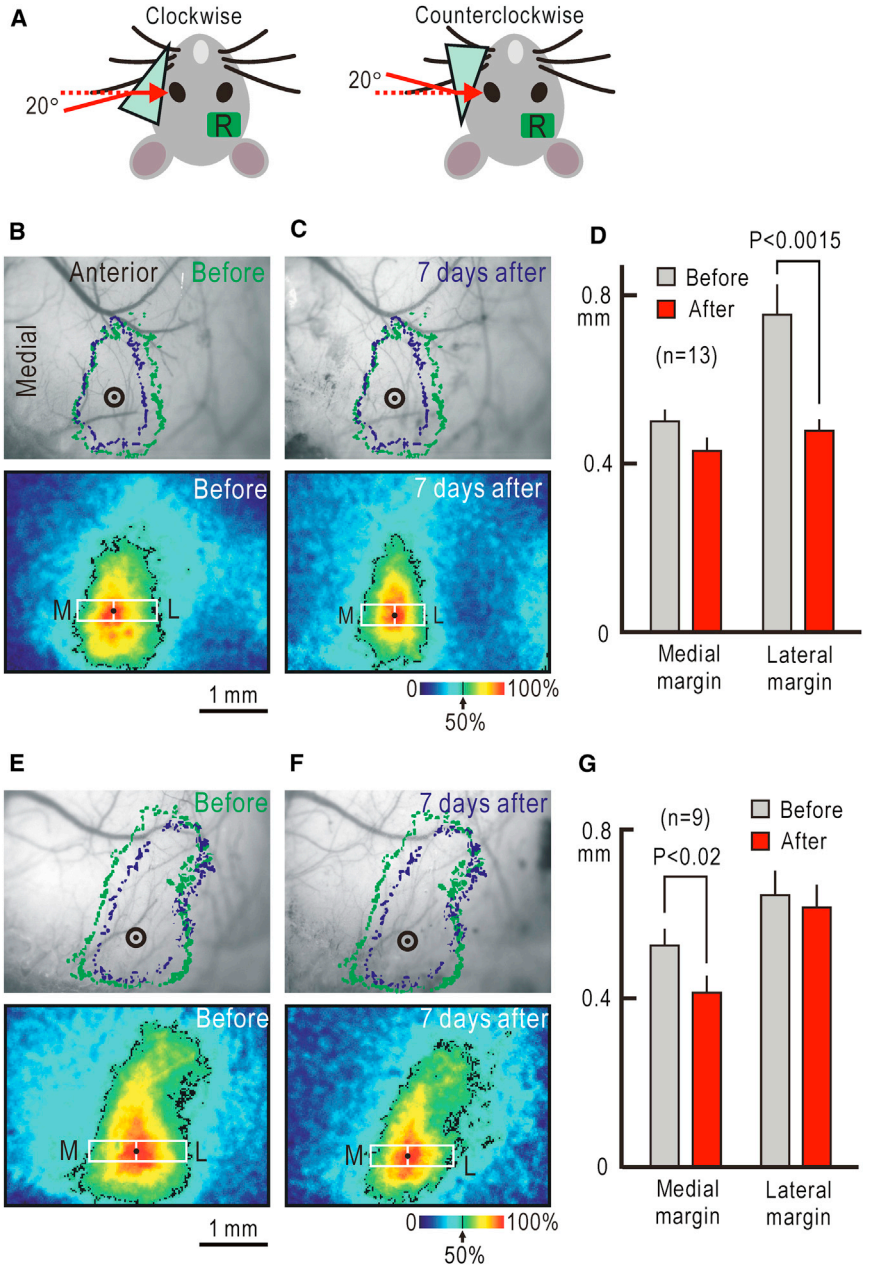

Figure 6. Comparison of Visual Responses before and after Prism Wearing in the Same Mice

(A) Prism goggle attached to the head of mice for 7 days between 4 weeks and 5 weeks of age. This goggle was designed to produce a clockwise or counterclockwise rotation of the light path to V1M by 20°.

(B) Original image (upper panel) and image of $\Delta F/F_0$ obtained by Fourier analysis (lower panel) before wearing the prism goggle that produced a clockwise rotation of the light path to V1M by 20°. The pixel with the maximal $\Delta F/F_0$ is marked with a black spot with or without a circle, and pixels with half the maximal $\Delta F/F_0$ are marked with black dots in the lower panel and green dots in the upper panel. Blue dots in the upper panel represent the pixels with half the maximal $\Delta F/F_0$ after prism wearing in the same mouse. The white rectangles in the lower panel show the medial (M) and lateral margins (L) of the response area, measured within 0.3 mm including the pixel with the maximal $\Delta F/F_0$.

(C) Original image (upper panel) and image of $\Delta F/F_0$ obtained by Fourier analysis (lower panel) after prism wearing in the same mouse.

(D) Medial and lateral margins of the response area before and after prism wearing.

(E) Original image (upper panel) and image of $\Delta F/F_0$ obtained by Fourier analysis (lower panel) before wearing the prism goggle that produced a counterclockwise rotation of the light path to V1M by 20°.

(F) Original image (upper panel) and image of $\Delta F/F_0$ obtained by Fourier analysis (lower panel) after prism wearing in the same mouse.

(G) Medial and lateral margins of the response area before and after prism wearing.

See also Figure S6.

The prism-induced cortical depression could be observed as a shrinkage of the response area, as well as a reduction in response amplitudes. We compared cortical activity in V1 before and after prism wearing in the same mice, as described in our previous study with regard to ocular dominance plasticity after MD (Tohmi et al., 2006). However, we could not find the prism-induced depression in mice recovered from urethane anesthesia. This is probably because the prism-induced depression and map shifts require frequent mismatching between whisker and visual inputs during spatial navigation, although such mismatching only happened rarely in groggy and inactive mice recovered from urethane anesthesia. Therefore, we improved the previous technique in three ways. First, mice were anesthetized with a mixture of urethane and pentobarbital because this allowed them to recover from the anesthesia more quickly. Second, Fourier image analysis (Kalatsky and Stryker, 2003) was adopted so that imaging experiments could be completed within 20 min. Third, the periosteum covering the skull was kept intact to maintain the transparency of the skull

previous studies (Tohmi et al., 2006; Llano et al., 2009). Prism-induced depression was detected as changes in the activity of numerous V1 neurons. Two-photon calcium imaging (for example, see Figures S3E–S3G) might reveal the properties of many individual neurons at once. However, the magnitude of the calcium signals, which are strongly affected by the local distribution of calcium indicators, cannot be directly compared between different mice. We used flavoprotein fluorescence imaging in this study because the results obtained with this method can be compared between different mice, as shown in previous studies (Takahashi et al., 2006; Tohmi et al., 2006; Wang et al., 2009; Komagata et al., 2011; Yamashita et al., 2012).

during the whole course of the experiments. These improvements allowed us to compare the precise response areas in V1 before and after prism wearing in the same mice. The present findings clearly indicate that the improved method is a useful technique for demonstrating even slight experience-dependent shifts in the distribution of cortical activity in mice.

Comparison of Two Types of Cortical Plasticity in V1 after Prism Wearing or MD

The prism-induced cortical depression in the present study is different from ocular dominance plasticity after MD in several ways. First, prism-induced cortical depression was observed in V1M as well as in V1B, and binocular interactions are unlikely to be responsible for the prism-induced depression in V1M. The contribution of binocular interactions in V1B is also unlikely, since the prism-induced depression was abolished by whisker trimming in V1B as well as in V1M. Another unique property of the prism-induced depression is that it was blocked by lesions in a visuotactile association area in the PPC. The lesion that effectively blocked the prism-induced cortical depression was located in an area that is involved in spatial learning in rodents (Pinto-Hamuy et al., 2004; Rogers and Kesner, 2007; Torrealba and Valdés, 2008; Harvey et al., 2012). The critical period for the prism-induced depression was similar to that found for ocular dominance plasticity after MD, suggesting that both might share a part of the mechanisms and neural circuits. However, we found that the prism-induced depression (but not ocular dominant plasticity) after MD was abolished in Pcdh-α KO mice. In Pcdh-α KO mice, distribution of serotonergic fibers is abnormal (Katori et al., 2009). Although serotonergic fibers are required for developmental plasticity in V1 (Gu and Singer, 1995), ocular dominance plasticity after MD was found in mice with PPC lesions and in Pcdh-α KO mice, indicating that the serotonin level in V1 of these mice was sufficient to induce developmental plasticity. However, the formation of cortico-cortical pathways, which are likely to play a critical role in visuotactile sensory association, is impaired between the bilateral somatosensory cortices of Pcdh-α KO mice (Yamashita et al., 2012). Finally, cortical depression, map shifts, and reduced visual acuity were observed after prism wearing in a part of V1M that had not received the abnormal visual inputs that are usually required for the induction of notable developmental plasticity in V1. These unique properties of cortical plasticity after prism wearing clearly indicate that it is a type of developmental plasticity in V1.

Possible Modification of V1 Circuits in Prism-Induced Cortical Plasticity

Inhibitory neurons of specific types play critical roles in specific V1 functions (Wilson et al., 2012; Lee et al., 2012), including ocular dominance plasticity after MD (Maffei et al., 2006; Yazaki-Sugiyama et al., 2009). The critical period of ocular dominance plasticity is mainly determined by the functional maturation of inhibitory synapses (Hensch, 2005; Katagiri et al., 2007; Maffei et al., 2010), and the prism-induced cortical depression showed a critical period similar to that of ocular dominance plasticity after MD. Inhibitory neurons in V1 are partly driven by feedback input that originates from higher areas (Dong et al., 2004; Burkhalter, 2008). Therefore, time-locked visual input and feedback input to inhibitory neurons in V1 could induce cortical depression during prism wearing. However, simple depression alone cannot explain the map shifts, and some morphological changes of neural circuits might be induced after prism wearing, as reported in a study of auditory map plasticity in the barn owl (McBride et al., 2008). Neurons in the lateral geniculate nuclei (LGN) project onto V1, and experience-dependent pruning of the axonal arbor in LGN neurons is induced during the critical period of ocular dominance plasticity (Antonini and Stryker, 1993; Hata et al., 1999). Strabismus mimicked by prism wearing induced shrinkage in LGN neurons in young monkeys (Crawford and von Noorden, 1996), suggesting that axonal pruning of LGN neurons might be induced by prism wearing. In kittens wearing prism goggles, the distribution of optimal disparities in V1B neurons shifted in a direction that would tend to compensate for the prism-induced disparity (Shlaer, 1971; Shinkman et al., 1992). Therefore, the map shifts observed in the present study can also be explained by selective axonal pruning of LGN neurons.

Prism-Induced Cortical Plasticity in Mice and Prism Adaptation in Other Species

Visually guided reaching toward a target is disturbed when the visual field is shifted by prism wearing, but the reaching performance recovers with practice (prism adaptation; Harris, 1965). Prism adaptation involves short-term sensorimotor plasticity and long-term reorganization in the neural representation of space, and the PPC is responsible for these changes (Harris, 1965; Newport et al., 2006; Vesia et al., 2006; Luauté et al., 2009). In monkeys that wore reversing prism goggles for a few months, V1M neurons began to respond to stimuli presented not only in the contralateral visual field but also in the ipsilateral field, indicating that prism adaptation is mediated, at least in part, by a functional reorganization in V1 (Sugita, 1996; Tanaka et al., 2007). Prism adaptation has been extensively investigated as a rehabilitation tool for adult subjects with spatial neglect (Rossetti et al., 1998; Frassinetti et al., 2002; Nijboer et al., 2011); however, no cortical depression or map shifts in V1 have been reported in human subjects. Whiskers played a critical role in the prism-induced plasticity of mice during the critical period, whereas other prism adaptations were observed even in adults with no whiskers. Regardless of these differences, both prism adaption and the prism-induced plasticity in V1 include long-term reorganization in the neural representation of space, suggesting that both could share a part of the underlying neural circuits in the PPC.

Possible Visuotactile Association Area in the PPC

The PPC in rodents includes the anteromedial (AM), anterior (A), and rostrolateral (RL) visual areas (Torrealba and Valdés, 2008; Wang et al., 2011). These areas adjacent to V1 receive retinotopically organized synaptic inputs from V1 (Wang and Burkhalter, 2007) and are driven by visual input (Tohmi et al., 2009; Andermann et al., 2011; Marshel et al., 2011). Neurons in RL also respond to somatosensory stimuli (Olcese et al., 2013). In flavoprotein fluorescence imaging, visual responses in these areas appear in the peripheral part of V1, and no gap separates these responses from V1 responses (Tohmi et al., 2009).

However, the lesioned site that most effectively blocked the prism-induced cortical depression in the present study was clearly separated from V1 activity, with a substantial gap of no activity (Figure 3), indicating that the lesion was in the mediomedial (MM) visual area located between the AM area and the retrosplenial cortex (Wang and Burkhalter, 2007; Wang et al., 2011). Therefore, the MM area is one of the most likely areas for detecting visuotactile spatial misalignment in mice. Focal injuries are accompanied by a reorganization of the adjacent neuronal networks (Imbrosci et al., 2010), and the functional properties of MM neurons are not well known at present. The diameter of the lesioned site in the present study was approximately 1 mm, and some damage may have been produced in the retrosplenial cortex, which is related to spatial navigation in rodents (Cooper and Mizumori, 2001; Harker and Whishaw, 2002). The lesioned site in the present study is also very close to the area related to spatial working memory (Harvey et al., 2012). Furthermore, possible impairment of the visual information flow via the dorsal pathways to the retrosplenial cortex might be responsible for the impaired prism-induced cortical depression after MM lesioning. Regardless of these limitations in the lesion experiments, the prism-induced cortical depression may serve as a simple experimental model for elucidating the cellular and molecular mechanisms underlying cross-modal sensory functions in the mammalian brain.

EXPERIMENTAL PROCEDURES

The ethics committee of Niigata University approved the experimental protocols used in this study. C57BL/6 mice were used.

Imaging Experiments

For conventional imaging experiments, mice were anesthetized with urethane (1.6 g/kg, i.p.). Throughout the recordings, rectal temperature was kept at 38°C using a silicon rubber heater. The head of each mouse was fixed using a stereotaxic frame (SG-4; Narishige). Surgical procedures were conducted under sterile conditions. After subcutaneous injection of bupivacaine (AstraZeneca), disinfected skin was incised and the skull above V1 of both hemispheres was exposed. The surface of the intact skull was covered with a mixture of liquid paraffin and Vaseline to prevent drying and to keep the skull transparent. Surgical procedures were usually finished within 20 min. An additional dose of urethane (0.2 g/kg, s.c.) was administered when necessary. At the end of the imaging experiments, the mice were killed with an overdose of pentobarbital (i.p.).

Imaging was started about 1 hr after administration of urethane. Cortical images (128 × 168 pixels after binning) of endogenous green fluorescence (λ = 500–550 nm) in blue light (λ = 450–490 nm) were recorded in the area including V1 of both hemispheres at nine frames/s by a cooled CCD camera system (Aquacosmos system with an ORCA-ER camera; Hamamatsu Photonics). The camera was attached to a binocular epifluorescence microscope with a 75 W xenon light source (MZ FL III; Leica Microsystems). Fluorescence images were obtained in a recording session, during which the mice were given visual stimuli in trials repeated at 20 s intervals. Images elicited by a particular stimulus were averaged over 24 trials. Spatial moving averaging in areas of 5 × 5 pixels was used to improve image quality. Images were normalized, pixel by pixel, with respect to a reference image, which was obtained by averaging five images acquired immediately before stimulation. The normalized images are shown in a pseudocolor scale representing relative fluorescence changes ($\Delta F/F_0$). The response amplitude at 0.6–1.0 s after stimulus onset was evaluated as values of $\Delta F/F_0$ in a square window of 10 × 10 pixels. The location of the window was determined by a computer program, so that the response amplitude in $\Delta F/F_0$ was maximal. The location of a visual response was determined as that of a circular window (diameter: 10 or 20 pixels) at which $\Delta F/F_0$ was maximal. The sizes of the response area, in which $\Delta F/F_0$ was larger than half the maximal amplitude, were also measured. During the recording experiments, stimulated eyes were opened until the entire pupil was exposed. Corneas were repeatedly covered with saline throughout the experiments to prevent drying.

Visual Stimulation

As a visual stimulus, we used a red LED (λ, 613 nm; diameter, 3 mm; TLSH160 [F]; Toshiba), which was placed 30 cm away from the mouse in the horizontal plane. The LED was turned on for 1 s in each trial, and only on-responses were investigated. One of the two eyes was covered to enable stimulation of the uncovered eye only. LED stimuli were presented in front of the mice (0°) to stimulate responses in V1B, and on the left or right side of the mice (90°) to stimulate responses in V1M. When the fine locations of visual responses were investigated, the LED stimuli were placed between 0° and 100° at 20° intervals. As a second type of stimulus, moving grating patterns were produced by a visual stimulus generator (ViSaGe; Cambridge Research System) and shown on a liquid crystal display (20° × 20°) placed 30 cm away from the mice. To avoid perturbation of fluorescence measurements using blue and green lights, the surface of the monitor was covered with a filter passing red light with λ > 600 nm (Sharp Cut Filter; Kenko). Moving grating patterns of 0.2 cycle/° with a square wave contrast and speed at 5°/s were presented for 1 s in each trial. One of the eight directions at 45° intervals from 0° to 360° was randomly selected in each trial, and the results were averaged.

Field Potential Recording

Field potentials were recorded in seven mice after imaging experiments. A glass micropipette filled with a 2 M NaCl solution (1 MΩ) was used as the recording electrode. A small hole was made in the skull above the response center identified by imaging experiments, and the tip of the electrode was inserted to a depth of 400 μm from the pial surface. The field potentials recorded in 100 trials were averaged.

Fourier Image Analysis

To determine the shifts of visual response areas in V1 after prism wearing, we performed Fourier image analysis twice at an interval of 1 week in the same mice (Kalatsky and Stryker, 2003). A mixture of urethane and pentobarbital (0.6 g/kg and 30 mg/kg, i.p., respectively) was used to ensure quick recovery from anesthesia. Fradiomycin (Mochida Pharmaceutical) and ampicillin (Meiji Seika Pharma) were used to avoid infection. The periosteum covering the skull above V1 was kept intact, and the surface was covered with a transparent wrapping film to prevent drying during recording experiments. Imaging was started 20 min after administration of the mixture of urethane and pentobarbital, and finished within 20 min. A red LED placed at 90° on the left side of the mice was turned on for 1 s at 0.25 Hz between 100 and 200 times. The signal amplitude in $\Delta F/F_0$ modulated at 0.25 Hz was extracted in each pixel using Fourier analysis. The response center, at which the maximal $\Delta F/F_0$ was recorded, and the margin of the response area, at which the half-maximal $\Delta F/F_0$ was recorded, were determined by a computer program. After the first imaging session (performed at 4 weeks of age) was finished, the transparent wrapping film was removed and a prism goggle was attached to the mouse's skull. The skin covering the skull was sutured before the mouse recovered from anesthesia. After the second imaging session (performed at 5 weeks of age) was finished, the mice were killed with an overdose of pentobarbital.

Procedures for Modulating Cortical Plasticity

Surgical procedures to produce cortical plasticity or cortical lesions were conducted in mice under anesthesia with pentobarbital (60 mg/kg, i.p.). Fradiomycin and ampicillin were used to avoid infection. A clear acryl prism goggle weighing 0.6 g was attached to the skull with acrylic dental resin (Super bond; Sun Medical). When MD was performed, the skin around one eye was disinfected with 70% alcohol. Eyelids were sutured with a fine surgical nylon thread (diameter: 0.23 mm; Mani). During MD, the mice were checked daily to ensure that their eyes remained closed and uninfected. An ophthalmic solution containing levofloxacin (5 mg/ml; Santen Pharmaceutical) was applied to the sutured eye every day. A cortical lesion was made by passing direct currents (0.2 mA, 1 s) through a metal electrode, the tip of which was inserted into

the cortex to a depth of 0.5 mm from the surface through a hole in the skull. The hole was sealed with acrylic dental resin after the lesion was made.

Statistical Analysis

Statistical significances in the data were analyzed using StatView software (SAS Institute). Paired data obtained from the same mice were evaluated by the Wilcoxon signed-rank test. Unpaired data obtained from different mice were evaluated by the Mann-Whitney U test. Only p values < 0.05 are shown.

SUPPLEMENTAL INFORMATION

Supplemental Information includes Supplemental Experimental Procedures and six figures and can be found with this article online at http://dx.doi.org/10.1016/j.celrep.2013.11.006.

ACKNOWLEDGMENTS

We thank Y. Maeda, M. Yokoyama, Y. Tamura, S. Maruyama, and A. Matsushima for their technical assistance. This work was supported by a Grant-in-Aid for Scientific Research (22115011).

Received: April 9, 2013
Revised: October 3, 2013
Accepted: November 4, 2013
Published: December 5, 2013

REFERENCES

Andermann, M.L., Kerlin, A.M., Roumis, D.K., Glickfeld, L.L., and Reid, R.C. (2011). Functional specialization of mouse higher visual cortical areas. Neuron *72*, 1025–1039.

Andersen, R.A. (1997). Multimodal integration for the representation of space in the posterior parietal cortex. Philos. Trans. R. Soc. Lond. B Biol. Sci. *352*, 1421–1428.

Antonini, A., and Stryker, M.P. (1993). Rapid remodeling of axonal arbors in the visual cortex. Science *260*, 1819–1821.

Bavelier, D., and Neville, H.J. (2002). Cross-modal plasticity: where and how? Nat. Rev. Neurosci. *3*, 443–452.

Burkhalter, A. (2008). Many specialists for suppressing cortical excitation. Front Neurosci. *2*, 155–167.

Cooper, B.G., and Mizumori, S.J. (2001). Temporary inactivation of the retrosplenial cortex causes a transient reorganization of spatial coding in the hippocampus. J. Neurosci. *21*, 3986–4001.

Crawford, M.L., and von Noorden, G.K. (1996). Shrinkage and recovery of cells of the lateral geniculate nuclei with prism-rearing in macaques. Behav. Brain Res. *79*, 233–238.

Diamond, M.E., von Heimendahl, M., Knutsen, P.M., Kleinfeld, D., and Ahissar, E. (2008). 'Where' and 'what' in the whisker sensorimotor system. Nat. Rev. Neurosci. *9*, 601–612.

Dong, H., Shao, Z., Nerbonne, J.M., and Burkhalter, A. (2004). Differential depression of inhibitory synaptic responses in feedforward and feedback circuits between different areas of mouse visual cortex. J. Comp. Neurol. *475*, 361–373.

Frassinetti, F., Angeli, V., Meneghello, F., Avanzi, S., and Làdavas, E. (2002). Long-lasting amelioration of visuospatial neglect by prism adaptation. Brain *125*, 608–623.

Gordon, J.A., and Stryker, M.P. (1996). Experience-dependent plasticity of binocular responses in the primary visual cortex of the mouse. J. Neurosci. *16*, 3274–3286.

Gu, Q., and Singer, W. (1995). Involvement of serotonin in developmental plasticity of kitten visual cortex. Eur. J. Neurosci. *7*, 1146–1153.

Harker, K.T., and Whishaw, I.Q. (2002). Impaired spatial performance in rats with retrosplenial lesions: importance of the spatial problem and the rat strain in identifying lesion effects in a swimming pool. J. Neurosci. *22*, 1155–1164.

Harris, C.S. (1965). Perceptual adaptation to inverted, reversed, and displaced vision. Psychol. Rev. *72*, 419–444.

Harvey, C.D., Coen, P., and Tank, D.W. (2012). Choice-specific sequences in parietal cortex during a virtual-navigation decision task. Nature *484*, 62–68.

Hata, Y., Tsumoto, T., and Stryker, M.P. (1999). Selective pruning of more active afferents when cat visual cortex is pharmacologically inhibited. Neuron *22*, 375–381.

Hensch, T.K. (2005). Critical period plasticity in local cortical circuits. Nat. Rev. Neurosci. *6*, 877–888.

Hess, R.F., Thompson, B., Gole, G.A., and Mullen, K.T. (2010). The amblyopic deficit and its relationship to geniculo-cortical processing streams. J. Neurophysiol. *104*, 475–483.

Imbrosci, B., Eysel, U.T., and Mittmann, T. (2010). Metaplasticity of horizontal connections in the vicinity of focal laser lesions in rat visual cortex. J. Physiol. *588*, 4695–4703.

Kalatsky, V.A., and Stryker, M.P. (2003). New paradigm for optical imaging: temporally encoded maps of intrinsic signal. Neuron *38*, 529–545.

Katagiri, H., Fagiolini, M., and Hensch, T.K. (2007). Optimization of somatic inhibition at critical period onset in mouse visual cortex. Neuron *53*, 805–812.

Katori, S., Hamada, S., Noguchi, Y., Fukuda, E., Yamamoto, T., Yamamoto, H., Hasegawa, S., and Yagi, T. (2009). Protocadherin-alpha family is required for serotonergic projections to appropriately innervate target brain areas. J. Neurosci. *29*, 9137–9147.

Knudsen, E.I. (2002). Instructed learning in the auditory localization pathway of the barn owl. Nature *417*, 322–328.

Kohmura, N., Senzaki, K., Hamada, S., Kai, N., Yasuda, R., Watanabe, M., Ishii, H., Yasuda, M., Mishina, M., and Yagi, T. (1998). Diversity revealed by a novel family of cadherins expressed in neurons at a synaptic complex. Neuron *20*, 1137–1151.

Komagata, S., Chen, S., Suzuki, A., Yamashita, H., Hishida, R., Maeda, T., Shibata, M., and Shibuki, K. (2011). Initial phase of neuropathic pain within a few hours after nerve injury in mice. J. Neurosci. *31*, 4896–4905.

Konishi, M. (2003). Coding of auditory space. Annu. Rev. Neurosci. *26*, 31–55.

Kubota, Y., Kamatani, D., Tsukano, H., Ohshima, S., Takahashi, K., Hishida, R., Kudoh, M., Takahashi, S., and Shibuki, K. (2008). Transcranial photo-inactivation of neural activities in the mouse auditory cortex. Neurosci. Res. *60*, 422–430.

Lee, S.H., Kwan, A.C., Zhang, S., Phoumthipphavong, V., Flannery, J.G., Masmanidis, S.C., Taniguchi, H., Huang, Z.J., Zhang, F., Boyden, E.S., et al. (2012). Activation of specific interneurons improves V1 feature selectivity and visual perception. Nature *488*, 379–383.

Lewald, J., Peters, S., Tegenthoff, M., and Hausmann, M. (2009). Distortion of auditory space in hemianopia. Eur. J. Neurosci. *30*, 1401–1411.

Llano, D.A., Theyel, B.B., Mallik, A.K., Sherman, S.M., and Issa, N.P. (2009). Rapid and sensitive mapping of long-range connections in vitro using flavoprotein autofluorescence imaging combined with laser photostimulation. J. Neurophysiol. *101*, 3325–3340.

Luauté, J., Schwartz, S., Rossetti, Y., Spiridon, M., Rode, G., Boisson, D., and Vuilleumier, P. (2009). Dynamic changes in brain activity during prism adaptation. J. Neurosci. *29*, 169–178.

Maffei, L., and Bisti, S. (1976). Binocular interaction in strabismic kittens deprived of Vision. Science *191*, 579–580.

Maffei, A., Nataraj, K., Nelson, S.B., and Turrigiano, G.G. (2006). Potentiation of cortical inhibition by visual deprivation. Nature *443*, 81–84.

Maffei, A., Lambo, M.E., and Turrigiano, G.G. (2010). Critical period for inhibitory plasticity in rodent binocular V1. J. Neurosci. *30*, 3304–3309.

Maravita, A., Spence, C., and Driver, J. (2003). Multisensory integration and the body schema: close to hand and within reach. Curr. Biol. *13*, R531–R539.

Marshel, J.H., Garrett, M.E., Nauhaus, I., and Callaway, E.M. (2011). Functional specialization of seven mouse visual cortical areas. Neuron *72*, 1040–1054.

McBride, T.J., Rodriguez-Contreras, A., Trinh, A., Bailey, R., and Debello, W.M. (2008). Learning drives differential clustering of axodendritic contacts in the barn owl auditory system. J. Neurosci. *28*, 6960–6973.

Mrsic-Flogel, T.D., Hofer, S.B., Ohki, K., Reid, R.C., Bonhoeffer, T., and Hübener, M. (2007). Homeostatic regulation of eye-specific responses in visual cortex during ocular dominance plasticity. Neuron *54*, 961–972.

Nataraj, K., and Turrigiano, G. (2011). Regional and temporal specificity of intrinsic plasticity mechanisms in rodent primary visual cortex. J. Neurosci. *31*, 17932–17940.

Newport, R., Brown, L., Husain, M., Mort, D., and Jackson, S.R. (2006). The role of the posterior parietal lobe in prism adaptation: Failure to adapt to optical prisms in a patient with bilateral damage to posterior parietal cortex. Cortex *42*, 720–729.

Nijboer, T.C., Nys, G.M., van der Smagt, M.J., van der Stigchel, S., and Dijkerman, H.C. (2011). Repetitive long-term prism adaptation permanently improves the detection of contralesional visual stimuli in a patient with chronic neglect. Cortex *47*, 734–740.

O'Leary, D.D., Ruff, N.L., and Dyck, R.H. (1994). Development, critical period plasticity, and adult reorganizations of mammalian somatosensory systems. Curr. Opin. Neurobiol. *4*, 535–544.

Ohki, K., Chung, S., Ch'ng, Y.H., Kara, P., and Reid, R.C. (2005). Functional imaging with cellular resolution reveals precise micro-architecture in visual cortex. Nature *433*, 597–603.

Olcese, U., Iurilli, G., and Medini, P. (2013). Cellular and synaptic architecture of multisensory integration in the mouse neocortex. Neuron *79*, 579–593.

Pinto-Hamuy, T., Montero, V.M., and Torrealba, F. (2004). Neurotoxic lesion of anteromedial/posterior parietal cortex disrupts spatial maze memory in blind rats. Behav. Brain Res. *153*, 465–470.

Rogers, J.L., and Kesner, R.P. (2007). Hippocampal-parietal cortex interactions: evidence from a disconnection study in the rat. Behav. Brain Res. *179*, 19–27.

Rossetti, Y., Rode, G., Pisella, L., Farné, A., Li, L., Boisson, D., and Perenin, M.T. (1998). Prism adaptation to a rightward optical deviation rehabilitates left hemispatial neglect. Nature *395*, 166–169.

Sawtell, N.B., Frenkel, M.Y., Philpot, B.D., Nakazawa, K., Tonegawa, S., and Bear, M.F. (2003). NMDA receptor-dependent ocular dominance plasticity in adult visual cortex. Neuron *38*, 977–985.

Sengpiel, F., Jirmann, K.U., Vorobyov, V., and Eysel, U.T. (2006). Strabismic suppression is mediated by inhibitory interactions in the primary visual cortex. Cereb. Cortex *16*, 1750–1758.

Shinkman, P.G., Timney, B., and Isley, M.R. (1992). Binocular depth perception following early experience with interocular torsional disparity. Vis. Neurosci. *9*, 303–312.

Shlaer, R. (1971). Shift in binocular disparity causes compensatory change in the cortical structure of kittens. Science *173*, 638–641.

Sugita, Y. (1996). Global plasticity in adult visual cortex following reversal of visual input. Nature *380*, 523–526.

Tagawa, Y., Kanold, P.O., Majdan, M., and Shatz, C.J. (2005). Multiple periods of functional ocular dominance plasticity in mouse visual cortex. Nat. Neurosci. *8*, 380–388.

Takahashi, K., Hishida, R., Kubota, Y., Kudoh, M., Takahashi, S., and Shibuki, K. (2006). Transcranial fluorescence imaging of auditory cortical plasticity regulated by acoustic environments in mice. Eur. J. Neurosci. *23*, 1365–1376.

Tanaka, Y., Miyauchi, S., Misaki, M., and Tashiro, T. (2007). Mirror symmetrical transfer of perceptual learning by prism adaptation. Vision Res. *47*, 1350–1361.

Tohmi, M., Kitaura, H., Komagata, S., Kudoh, M., and Shibuki, K. (2006). Enduring critical period plasticity visualized by transcranial flavoprotein imaging in mouse primary visual cortex. J. Neurosci. *26*, 11775–11785.

Tohmi, M., Takahashi, K., Kubota, Y., Hishida, R., and Shibuki, K. (2009). Transcranial flavoprotein fluorescence imaging of mouse cortical activity and plasticity. J. Neurochem. *109* (*Suppl 1*), 3–9.

Torrealba, F., and Valdés, J.L. (2008). The parietal association cortex of the rat. Biol. Res. *41*, 369–377.

Van Brussel, L., Gerits, A., and Arckens, L. (2011). Evidence for cross-modal plasticity in adult mouse visual cortex following monocular enucleation. Cereb. Cortex *21*, 2133–2146.

Van Essen, D.C., and Gallant, J.L. (1994). Neural mechanisms of form and motion processing in the primate visual system. Neuron *13*, 1–10.

Vesia, M., Monteon, J.A., Sergio, L.E., and Crawford, J.D. (2006). Hemispheric asymmetry in memory-guided pointing during single-pulse transcranial magnetic stimulation of human parietal cortex. J. Neurophysiol. *96*, 3016–3027.

Wang, Q., and Burkhalter, A. (2007). Area map of mouse visual cortex. J. Comp. Neurol. *502*, 339–357.

Wang, X., Chen, G., Gao, W., and Ebner, T. (2009). Long-term potentiation of the responses to parallel fiber stimulation in mouse cerebellar cortex *in vivo*. Neuroscience *162*, 713–722.

Wang, Q., Gao, E., and Burkhalter, A. (2011). Gateways of ventral and dorsal streams in mouse visual cortex. J. Neurosci. *31*, 1905–1918.

Wilson, N.R., Runyan, C.A., Wang, F.L., and Sur, M. (2012). Division and subtraction by distinct cortical inhibitory networks in vivo. Nature *488*, 343–348.

Yagi, T. (2013). Genetic basis of neuronal individuality in the mammalian brain. J. Neurogenet. *27*, 97–105.

Yamashita, H., Chen, S., Komagata, S., Hishida, R., Iwasato, T., Itohara, S., Yagi, T., Endo, N., Shibata, M., and Shibuki, K. (2012). Restoration of contralateral representation in the mouse somatosensory cortex after crossing nerve transfer. PLoS ONE *7*, e35676.

Yazaki-Sugiyama, Y., Kang, S., Câteau, H., Fukai, T., and Hensch, T.K. (2009). Bidirectional plasticity in fast-spiking GABA circuits by visual experience. Nature *462*, 218–221.

Zhang, B., Bi, H., Sakai, E., Maruko, I., Zheng, J., Smith, E.L., 3rd, and Chino, Y.M. (2005). Rapid plasticity of binocular connections in developing monkey visual cortex (V1). Proc. Natl. Acad. Sci. USA *102*, 9026–9031.